

Synthesis of Nanostructured Cobalt Oxides using Cobalt(II) Fumarate Hydrate as Metal-Organic Precursor

M. GOGOI^{1,*} and B.K. DAS²

¹Department of Chemistry, Gauhati University, Guwahati-781014, India

²Department of Chemistry, Bhattadev University, Bajali, Pathsala-781325, India

*Corresponding author: E-mail: monsumigogoi@gmail.com

Received: 28 August 2020;

Accepted: 6 October 2020;

Published online: 7 December 2020;

AJC-20153

A series of nanostructured cobalt oxides have been prepared from a metal-organic precursor *viz.* [Co(fum)(H₂O)₄].H₂O (fum = fumarate) by using capping agents, ethylene glycol and polyethylene glycol *via* thermal and solvothermal decomposition in ethanol and also by doping with RuCl₃.xH₂O *via* solvothermal route. The nano oxides were characterized by IR, UV-vis spectroscopy, powder XRD, SEM and TEM analysis. The nano oxides exhibit varied morphologies and particle sizes. The TEM images reveal homogeneously distributed particles for all the oxides. The band gap energy values the Ru-doped cobalt oxide was found to be lower than the generally accepted values.

Keywords: Nano structure, Cobalt oxide, Cobalt(II) fumarate, Ruthenium, Solvothermal synthesis, Band gap.

INTRODUCTION

The nanostructured oxides of 3d transition metals have attracted significant interests due to their usefulness in various fields such as data storage devices, catalysis, drug delivery and biomedical imaging [1]. These have gained importance because of their good catalytic activity, selectivity and reusability. Nano particles show high surface to volume ratios and different chemical and physical properties compared with the bulk materials. Transition metal nano oxides are widely used in the field of heterogeneous catalysis. In particular, cobalt oxides nanocrystals are significant owing to their potential applications based on magnetic, catalytic and gas-sensing properties [2]. Co₃O₄ has applications in many fields, such as heterogeneous catalysts, electrochromic devices, solid-state sensors, energy storage and rotatable magnets. Co₃O₄ has a normal spinel structure in which Co²⁺ and Co³⁺ ions are at the centers of tetrahedral and octahedral sites, respectively. Numerous researches have been carried out on the synthesis and property investigation of Co₃O₄ nanomaterials [3-6]. Various kinds of morphologies for Co₃O₄ in nanometer scales have been successfully fabricated. These include morphologies like nanorods, nanospheres, hollow-nanospheres, nanocubes, nanotubes, *etc.* In recent years, significant advances have been made in the

synthesis of well defined nanostructured materials including metal oxides nanoparticles [7,8]. The most common and conventional synthetic route for the preparation of transition metal oxides are solution phase precipitation, sol-gel, solvothermal, thermolysis, *etc.* [9,10]. The shape, size, morphology and properties of the nanoparticles depend largely on several factors such as the identity and concentration of the precursor, reaction temperature, aging and on all other reaction conditions [11].

The synthetic route of the nanoparticles controls the various structural features such as average size, size distribution, close packing sequences and morphology. The capping agent, necessary to prevent merging and oxidation of the cobalt nano-oxides also play a crucial role. Capping agents can be used in colloidal synthesis to inhibit nanoparticle overgrowth and aggregation as well as to precisely control the structural characteristics of the synthesized nanoparticles. The residual capping agents on particle surface have unveiled various adverse and favourable behaviours in catalytic applications. Often they act as a physical barrier that obstructs the access of reactants to catalytic nanoparticles. However, they can also be utilized to promote catalytic performance of nanocrystals [12,13].

The precursor materials from where the nanoparticles are synthesized also play a decisive role in determining the particle size and morphology and even the physico-chemical properties

[14,15]. The most often used precursors include metal acetates, metal halides, metal salts and some other organometallic substances. Literature reports that most of the Co_3O_4 nanostructures have been prepared using both common cobalt salts and organo-cobalt precursors, following suitable preparative routes [16]. It may appear that the use of metal salts as the starting materials for the synthesis of Co_3O_4 nanostructures is more cost effective than that of using secondary precursor like organo-metallic complexes. But many instances suggest that the metal complexes can be used in a reproducible manner than the simple metal salts. This may provide better control on particle size, especially in the case of application oriented Co_3O_4 nanostructures.

In the present work, we describe the synthesis of nanostructured cobalt oxides from a well defined polymeric metal complex, viz. $[\text{Co}(\text{fum})(\text{H}_2\text{O})_4]\cdot\text{H}_2\text{O}$ which was reported earlier from this laboratory [17].

EXPERIMENTAL

All the chemicals used in this work were obtained from the commercial sources and used directly without further purification. All materials ethylene glycol, polyethylene glycol, $\text{RuCl}_3\cdot x\text{H}_2\text{O}$, sodium hydroxide purchased from E. Merck, India was used without further purification. Solvent used was of reagent grade.

General procedure

Synthesis of nanostructured cobalt oxides via precursor method: Previous work done in this laboratory involved the high-yield preparation and detailed characterization of many simple metal-organic compounds. Complexes of the type $[\text{M}(\text{O}_2\text{CR})_2(\text{OH}_2)_4]$ were shown to be good precursors to obtain binary metal oxides [18]. In this work, a cobalt(II) fumarate complex $[\text{Co}(\text{fum})(\text{H}_2\text{O})_4]\cdot\text{H}_2\text{O}$ has been used as the precursor for the synthesis of the nano structured Co_3O_4 . The metal-organic precursor is prepared following the procedure developed earlier in this laboratory [17]. Herein, we have made use of a NaOH neutralized fumaric acid solution instead of the solid form of sodium fumarate salt.

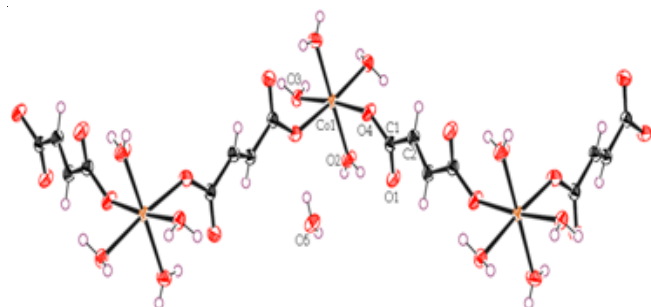


Fig. 1. A section of polymeric chain of the precursor complex $[\text{Co}(\text{fum})(\text{H}_2\text{O})_4]\cdot\text{H}_2\text{O}$

Cobalt(II) fumarate hydrate, when studied with thermogravimetry (TG) is found to undergo complete dehydration at $245\text{ }^\circ\text{C}$ and if heated beyond this temperature, the final residue is Co_3O_4 at $538\text{ }^\circ\text{C}$. This TG result has been utilized to prepare Co_3O_4 by using $[\text{Co}(\text{fum})(\text{H}_2\text{O})_4]\cdot\text{H}_2\text{O}$ as the precursor.

Synthesis of nanostructured Co_3O_4 by thermal decomposition

Synthesis of ethylene glycol capped Co_3O_4 : A mixture of NaOH solution (0.4 g in 50 mL H_2O), ethylene glycol (2 g $\approx 1.8018\text{ mL}$) and 20 mL ethanol was stirred for 15-30 min at room temperature. The metal complex, $[\text{Co}(\text{fum})(\text{H}_2\text{O})_4]\cdot\text{H}_2\text{O}$ (1 g) was added to the colourless solution and the stirring was continued for 30 min. The resultant black solution was then refluxed in oil bath at $120\text{ }^\circ\text{C}$ for about 2 h. The solution was then allowed to cool slowly at room temperature and centrifuging the solution separated the black precipitate so formed out. The black powder obtained was washed several times with water and dried in oven at $60\text{ }^\circ\text{C}$. The cobalt oxide so formed is named as $\text{EG}@\text{Co}_3\text{O}_4$.

Synthesis of polyethylene glycol capped Co_3O_4 : A mixture of NaOH solution (0.4 g in 50 mL H_2O), polyethylene glycol (2 g) and 20 mL ethanol was stirred for 15-30 min at room temperature. The metal complex, $[\text{Co}(\text{fum})(\text{H}_2\text{O})_4]\cdot\text{H}_2\text{O}$ (1 g) was added to the colourless solution and the stirring was continued for 30 min. The resultant black solution was then refluxed in oil bath at $140\text{ }^\circ\text{C}$ for about 2 h. The solution was then allowed to cool slowly at room temperature. The black precipitate so formed was separated out by centrifuging the solution. The black powder obtained was washed several times with water and dried in oven at $60\text{ }^\circ\text{C}$. The cobalt oxide so formed is named as $\text{PEG}@\text{Co}_3\text{O}_4\text{-1}$.

Synthesis of polyethylene-glycol capped Co_3O_4 via solvothermal route: A mixture of NaOH solution (0.2 g in 25 mL H_2O), polyethylene glycol (1 g) and 10 mL ethanol was stirred for 15-30 min at room temperature. The reaction solution immediately turns blood red on the addition of the metal complex, $[\text{Co}(\text{fum})(\text{H}_2\text{O})_4]\cdot\text{H}_2\text{O}$ (0.5 g). After 30 min of vigorous stirring, the reaction mixture was transferred into 100 mL Teflon-lined stainless autoclave which was then put in an oven at $140\text{ }^\circ\text{C}$ for 15 h and finally allowed to cool to room temperature naturally. The black precipitate so formed was separated out by centrifuging the solution. The black powder obtained was washed several times with water and finally once with ethanol and dried in oven at $60\text{ }^\circ\text{C}$. The cobalt oxide so formed is named as $\text{PEG}@\text{Co}_3\text{O}_4\text{-2}$.

Synthesis of ruthenium doped Co_3O_4 via solvothermal route: In a typical reaction, a mixture of NaOH solution (0.2 g in 25 mL H_2O) and the metal complex, $[\text{Co}(\text{fum})(\text{H}_2\text{O})_4]\cdot\text{H}_2\text{O}$ (1.55 g) was stirred for 30 min at room temperature. The reaction solution immediately turns black and to it, 5 mL ethanolic solution of a Ru salt ($\text{RuCl}_3\cdot x\text{H}_2\text{O}$) was added and stirred further for 1 h. A black product was obtained by removing the solvent at $85\text{ }^\circ\text{C}$, which was finally calcined at $400\text{ }^\circ\text{C}$ for 2 h and washed several times to make it chloride free. The cobalt oxide so formed is named as $\text{Ru}@\text{Co}_3\text{O}_4$.

Detection method: Diffuse reflectance UV-vis-NIR spectra (DRS) have been obtained by using a Hitachi U- 4100 spectrophotometer. BaSO_4 powder was used as reference (100% reflectance). From the reflectance data using the Kubelka-Munk function ($a/S = (1-R)^2/2R$ where 'a' is the absorption coefficient, 'R' the reflectance and 'S' the scattering coefficient), absorption data were calculated from the reflectance data. The IR spectra ($4000\text{-}240\text{ cm}^{-1}$) of the complexes were recorded as KBr disc

by using Shimadzu FT-IR spectrophotometer. X-ray powder diffraction pattern of the synthesized oxide samples were recorded using Philips X'pert Pro X-ray diffractometer with Cu-K α radiation ($\lambda = 1.5418 \text{ \AA}$) with 2θ ranging from 10 to 80° (wide angle) with a 0.05° steps and speed equal to $1^\circ/\text{min}$. The SEM images were obtained with a field emission scanning electron microscope (FESEM, SIGMA, Zeiss, Germany). Transmission electron microscopic (TEM) images were taken on a JEM-2100 instrumentation equipped with a high resolution CCD camera and at an accelerating voltage in the 60-100 kV range.

RESULTS AND DISCUSSION

Synthesis and characterization: As described in the experimental section, we have made use of the metal-organic species '[Co(fum)(H $_2$ O) $_4$]\cdot H $_2$ O', *i.e.*, cobalt(II) fumarate hydrate as the precursor for the synthesis of nanostructured oxides of cobalt. The metal fumarate based method developed by us for the synthesis of Co $_3$ O $_4$ has several advantages over the existing methods reported elsewhere. For this purpose we have explored several procedures for obtaining the oxide material under a variety of condition so that in due course it becomes possible on our part to examine if the synthesis conditions can influence the size and shape of the oxide particles.

Powder X-ray diffraction (XRD): All of the synthesized materials were primarily investigated by powder XRD that is known as the best technique to study the crystallographic phases and other structural parameters of crystalline materials. Then, other techniques like TEM, SEM, EDS *etc.* were used to characterize the materials in detail. The XRD patterns of the synthesized EG@Co $_3$ O $_4$, PEG@Co $_3$ O $_4$ -1 and PEG@Co $_3$ O $_4$ -2 (Fig. 2) are compared with that of the phase-pure Co $_3$ O $_4$ (JCPDS, Ref. No. 71-0816). It can be seen from the Fig. 2a-c that all the synthesized capped Co $_3$ O $_4$ materials exhibit three distinct peaks at the 2θ values of 37.02 , 59.67 and 65.57° which correspond to the (311), (400), (511) and (440) reflections of pure Co $_3$ O $_4$. Similarly, the diffractogram of the Ru deposited material (Fig. 3) can also be indexed to Co $_3$ O $_4$. The additional less intense peaks that appear at the 2θ value of 33.43 and 57.59 in the diffractogram is for Ru.

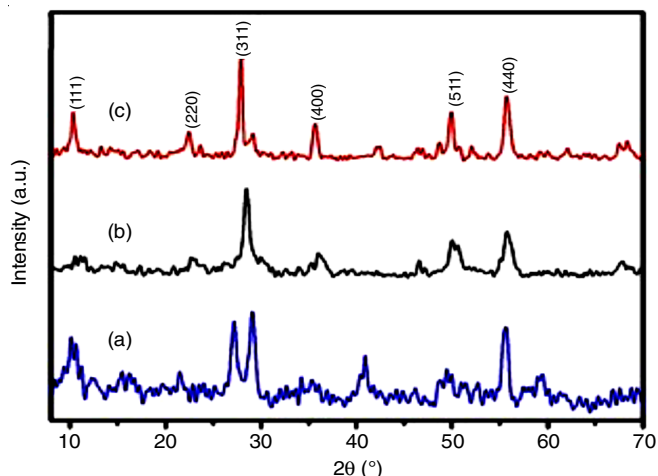


Fig. 2. X-ray diffractogram of (a) EG@Co $_3$ O $_4$, (b) PEG@Co $_3$ O $_4$ -1 and (c) PEG@Co $_3$ O $_4$ -2

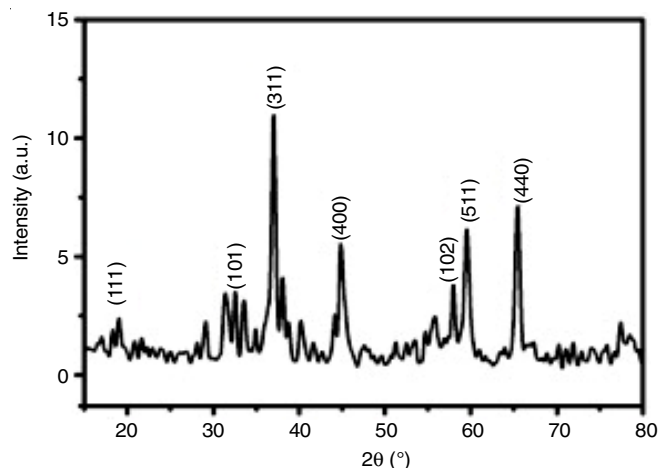


Fig. 3. X-ray diffractogram of Ru@Co $_3$ O $_4$

Electron microscopy (TEM and SEM): The TEM and HRTEM images of PEG@Co $_3$ O $_4$ -1 and PEG@Co $_3$ O $_4$ -2 are shown in Figs. 4 and 5 respectively from which it has been found that the average diameter of the oxide grains lie in the range of 6-8 nm and also that the particles are homogeneously distributed.

The morphological characteristics of the ethylene glycol and polyethylene glycol capped Co $_3$ O $_4$ were studied by scanning electron microscopy (SEM). Fig. 6a displays the agglomerated morphology of the EG@Co $_3$ O $_4$, while Fig. 6b-c shows that the particles of the PEG@Co $_3$ O $_4$ -1 and PEG@Co $_3$ O $_4$ -2 are spherical in shape.

The TEM image (Fig. 7) shows that the average particle size of Ru@Co $_3$ O $_4$ is 5 nm and also that the particles are homogeneously distributed. The SEM image of Ru@Co $_3$ O $_4$ (Fig. 8) shows the grass shaped morphology of the particles.

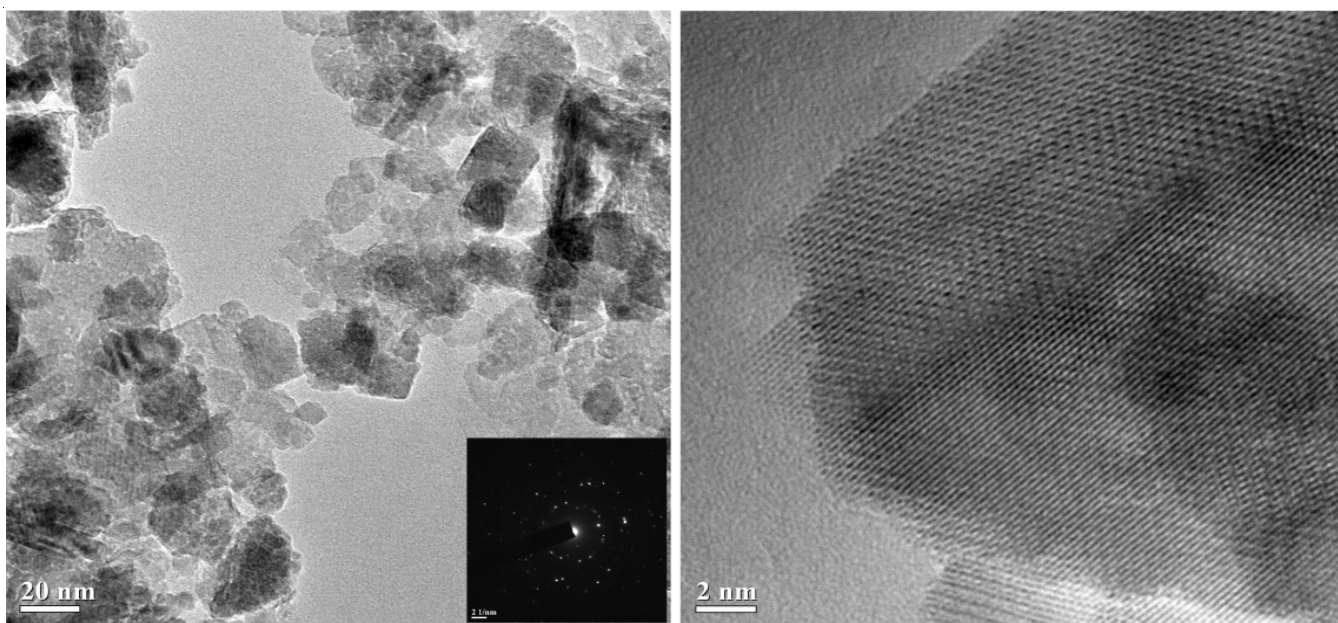
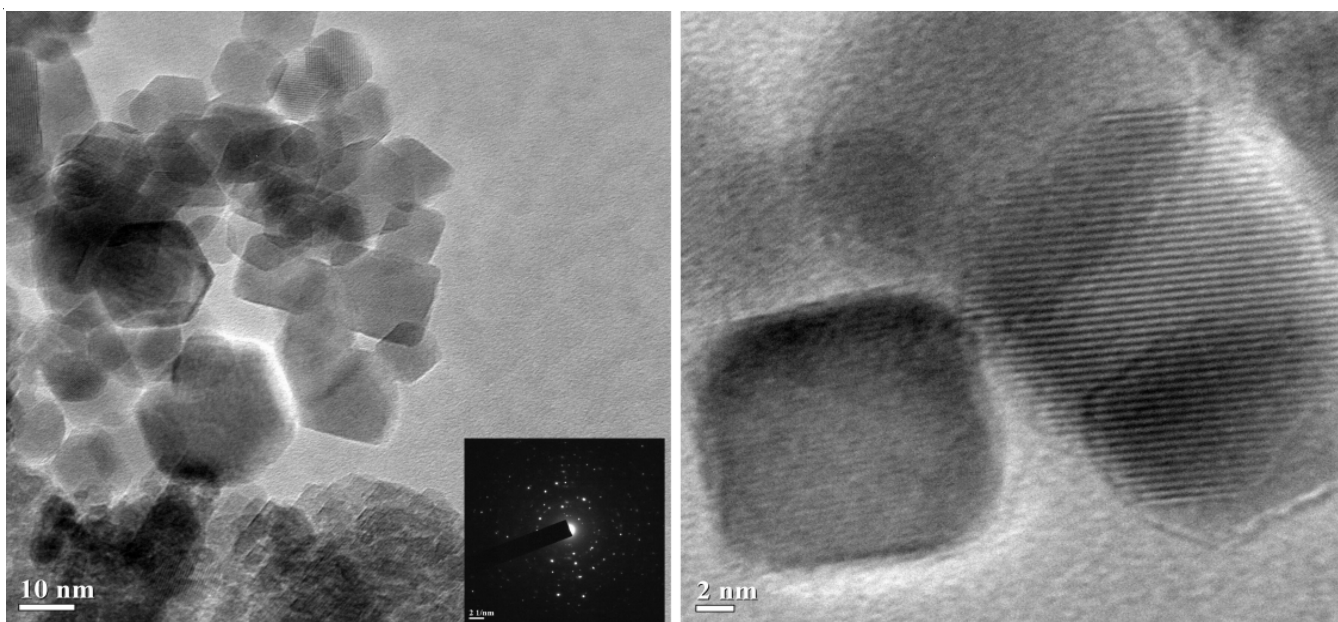
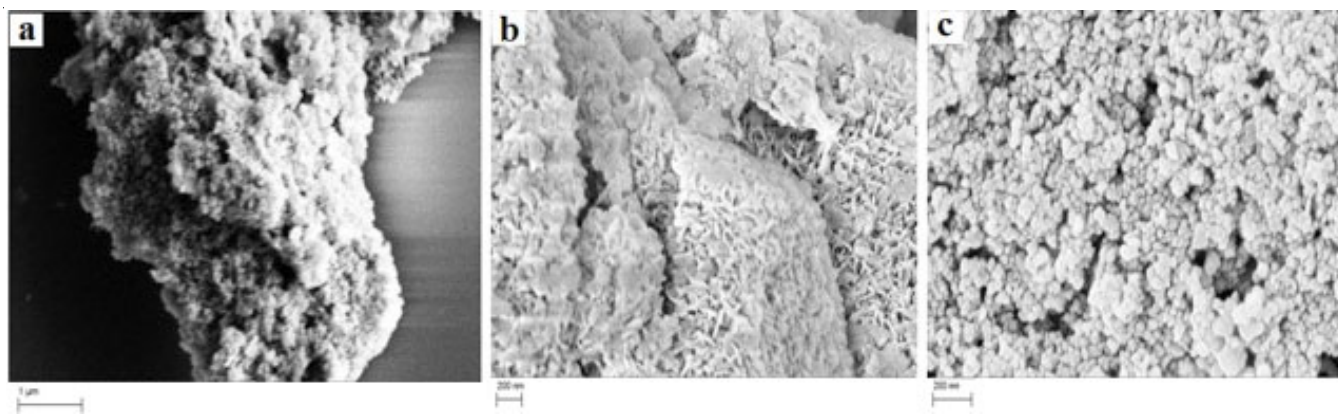
Energy dispersive X-ray spectroscopy (EDX): The EDX spectra provide complementary information about the composition of the materials. As shown in Fig. 9, both cobalt and ruthenium are present in the synthesized Ru@Co $_3$ O $_4$. The weight and atomic percentage composition of cobalt and ruthenium are listed in Table-1.

TABLE-1
PERCENTAGE COMPOSITION OF Co AND Ru IN Ru@Co $_3$ O $_4$

Element	Weight (%)	Atomic (%)
Cobalt	35.42	13.46
Ruthenium	1.21	0.27

Infrared spectral study: The FTIR spectra, in the mid-IR region, of all the synthesized Co $_3$ O $_4$ materials are presented from Figs. 10 and 11. All the seven oxide samples, exhibit two strong absorptions around 3440 and 1620 cm^{-1} which can be assigned to OH stretching or HOH bending vibrations of adsorbed moisture respectively. Two absorptions around 670 and 560 cm^{-1} have been observed for all the samples, which can be attributed to the Co-O vibration of Co $_3$ O $_4$ [19].

Diffuse reflectance spectra: The diffuse reflectance UV-vis (DRS-UV-Vis) absorption spectra of the cobalt oxide nanoparticles are presented in Figs. 12 and 13. The peak around 1.79 eV (typical for Co II in tetrahedral coordination) and a

Fig. 4. HRTEM images of PEG@Co₃O₄-1Fig. 5. HRTEM images of PEG@Co₃O₄-2Fig. 6. SEM images of (a) EG@Co₃O₄, (b) PEG@Co₃O₄-1 and (c) PEG@Co₃O₄-2

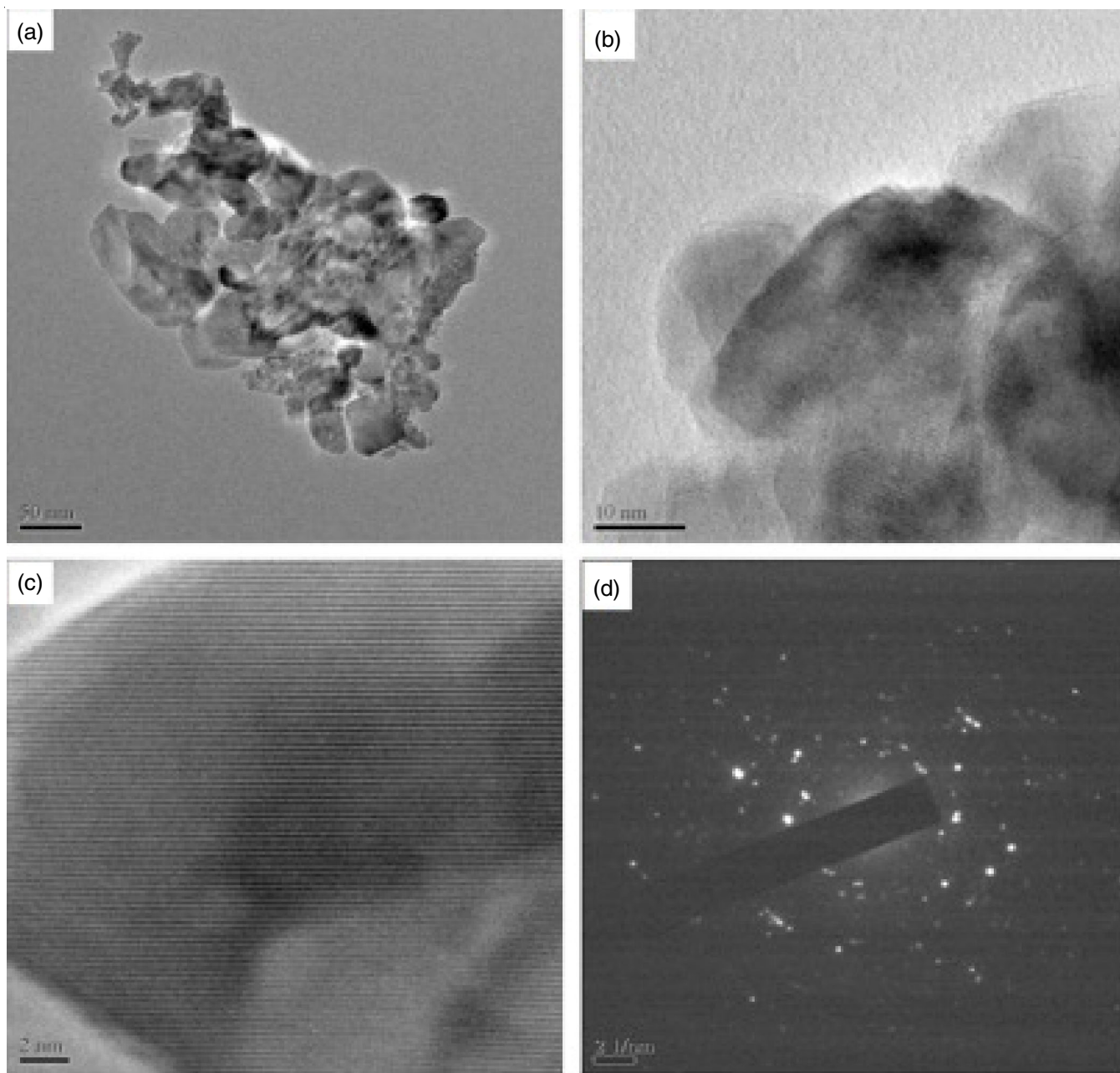


Fig. 7. (a,b) TEM images (c) HRTEM image and (d) SAED pattern of Ru@Co₃O₄

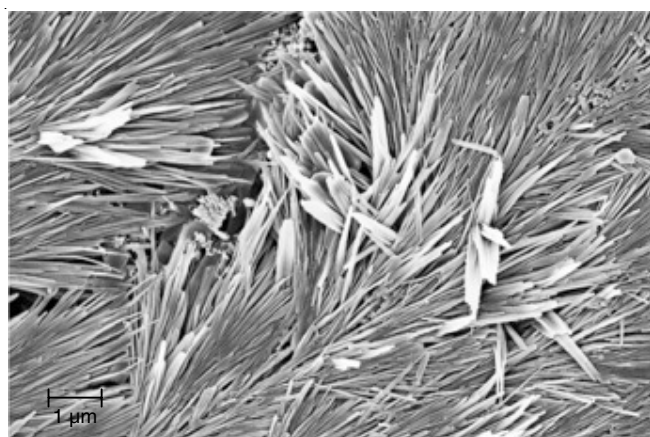


Fig. 8. SEM image of Ru@Co₃O₄

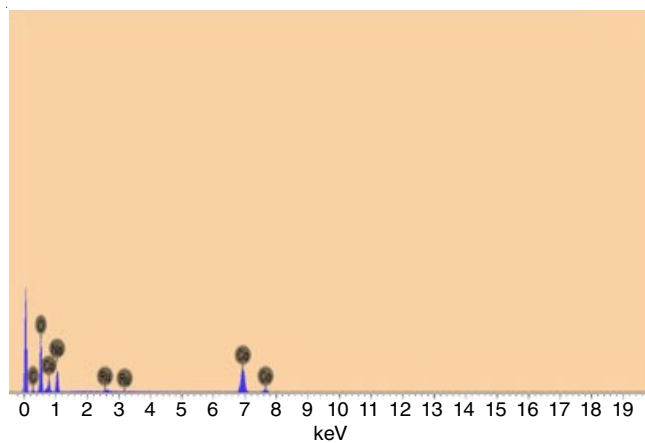
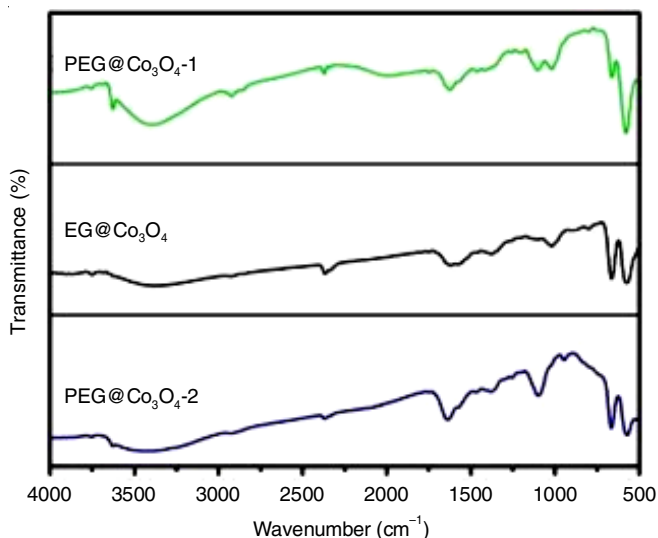
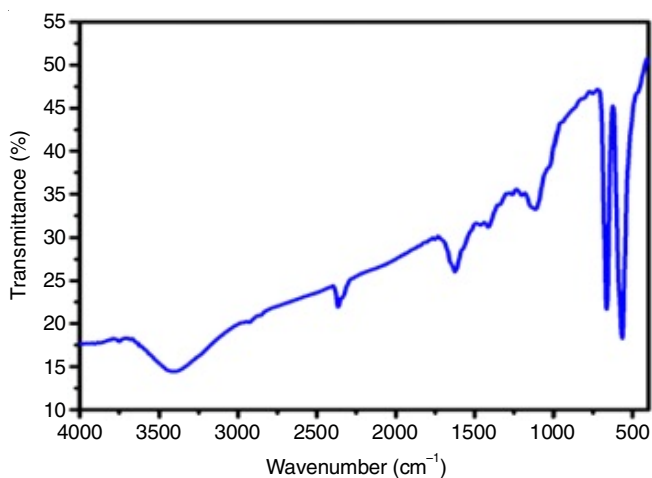
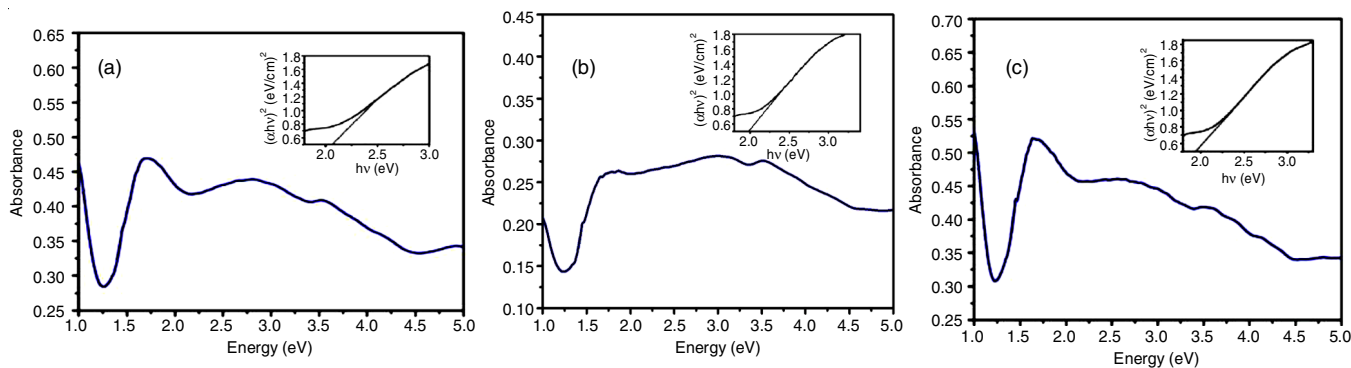
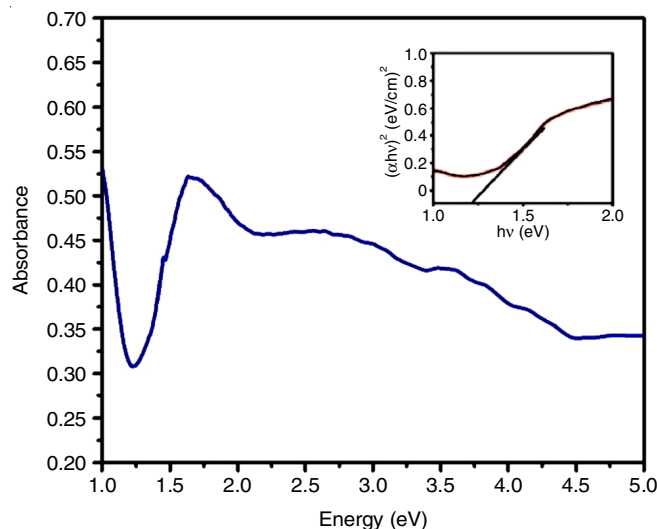


Fig. 9. EDX spectra of Ru@Co₃O₄

Fig. 10. FTIR spectra of EG@Co₃O₄, PEG@Co₃O₄-1 and PEG@Co₃O₄-2Fig. 11. FTIR spectrum of Ru@Co₃O₄

broad absorption within the vicinity of 2.59 eV (typical for Co^{III} in octahedral coordination) indicates that the synthesized oxide is spinel Co₃O₄ in which Co metal is in two different oxidation states *viz.* Co(II) and Co(III) [20].

The band gap energy values of the synthesized EG@Co₃O₄, PEG@Co₃O₄-1 and PEG@Co₃O₄-2 (Fig. 12a-c) are found to be 2.06, 1.99 and 1.94 eV, respectively, which are in good agreement with the generally accepted values [21,22].

Fig. 12. UV-vis diffuse reflectance spectra of (a) EG@Co₃O₄, (b) PEG@Co₃O₄-1 and (c) PEG@Co₃O₄-2, inset showing the $(\alpha hv)^2$ vs. hv plotFig. 13. UV-vis diffuse reflectance spectrum of Ru@Co₃O₄, inset showing the $(\alpha hv)^2$ vs. hv plot

The DR UV-vis spectrum of Ru@Co₃O₄ is shown in Fig. 13, from which its band gap energy value is found to be 1.22 eV, lowest of all the Co₃O₄ materials synthesized in this work. The optical band gaps of the nanomaterials have been evaluated following the Tauc's relationship, which is described as:

$$(\alpha hv)^{1/2} = C(hv - E_g)$$

where, α is the absorption coefficient of the semiconducting materials at a certain wavelength value λ , h is Planck's constant, C is a proportionality constant, v is the frequency of incident light, E_g is the band gap energy and the exponent, $n = 1/2$ and 2 for direct and indirect band gap respectively. The absorption coefficient (α) can be obtained from the equation:

$$\alpha = -\frac{1}{t} \ln \left(\frac{I_t}{I_0} \right) = \frac{1}{t} A \log e$$

where A , t , I_t and I_0 represent the absorbance, thickness of the nanomaterials film, intensity of transmitted light and intensity of incident light, respectively.

Conclusion

We have prepared a series of Co₃O₄ nanostructures with different morphologies (rod, spherical and grass like) by using the metal organic precursor, [Co(fum)(H₂O)₄].H₂O *via* solvo-thermal and thermal decomposition routes. The produced Co₃O₄

were characterized by XRD, SEM, TEM, EDS, *etc.* The average diameter of the oxide grain has been found in the range of 5–12 nm. The SAED pattern suggests the highly crystalline nature and the crystallinity of the oxides decreases with decrease in calcination temperature. The band gap energy values of Ru@Co₃O₄ are found to be the range of 1.22 eV. This low band gap value of the nanoparticles (≤ 1.5 eV), is relevant with semi-conducting property and thus these can be useful for photocatalysis.

ACKNOWLEDGEMENTS

The analytical services of SAIF NEHU, Shillong, IIT Indore and CIF, IASST, Guwahati, India are gratefully acknowledged.

CONFLICT OF INTEREST

The authors declare that there is no conflict of interests regarding the publication of this article.

REFERENCES

1. P. Walter, E. Welcomme, P. Hallegot, N.J. Zaluzec, C. Deeb, J. Castaing, P. Veyssiere, R. Breniaux, J.-L. Leveque and G. Tsoucaris, *Nano Lett.*, **6**, 2215 (2006); <https://doi.org/10.1021/nl061493u>
2. J. Zhu, K. Kailasam, A. Fischer and A. Thomas, *ACS Catal.*, **1**, 342 (2011); <https://doi.org/10.1021/cs100153a>
3. M. Reibold, P. Paufler, A.A. Levin, W. Kochmann, N. Patzke and D.C. Meyer, *Nature*, **444**, 286 (2006); <https://doi.org/10.1038/444286a>
4. L. Sciortino, A. Longo, F. Giannici and A. Martorana, *J. Phys.: Conf. Ser.*, **190**, 012125 (2009); <https://doi.org/10.1088/1742-6596/190/1/012125>
5. G. Schmid, *Endeavour*, **14**, 172 (1990); [https://doi.org/10.1016/0160-9327\(90\)90040-X](https://doi.org/10.1016/0160-9327(90)90040-X)
6. K.P. Gable and T.N. Phan, *J. Am. Chem. Soc.*, **116**, 833 (1994); <https://doi.org/10.1021/ja00082a002>
7. J. Tao, M.L. Tong, J.X. Shi, X.M. Chen and S. Ng, *Chem. Commun.*, **20**, 2043 (2000); <https://doi.org/10.1039/b005753n>
8. K.W. Chi, C. Addicott, A.M. Arif and P.J. Stang, *J. Am. Chem. Soc.*, **126**, 16569 (2004); <https://doi.org/10.1021/ja045542i>
9. T. Hyeon, *Chem. Commun.*, **120**, 927 (2003); <https://doi.org/10.1039/b207789b>
10. L. Hu, Q. Peng and Y. Li, *J. Am. Chem. Soc.*, **130**, 16136 (2008); <https://doi.org/10.1021/ja806400e>
11. I. Panagiotopoulos, V. Alexandrakis, G. Basina, S. Pal, H. Srikanth, D. Niarchos, G. Hadjipanayis and V. Tzitzios, *Cryst. Growth Des.*, **9**, 3353 (2009); <https://doi.org/10.1021/cg8006487>
12. J. Feng and H.C. Zeng, *Chem. Mater.*, **15**, 2829 (2003); <https://doi.org/10.1021/cm020940d>
13. T. He, D. Chen, X. Jiao, Y. Xu and Y. Gu, *Langmuir*, **20**, 8404 (2004); <https://doi.org/10.1021/la0488710>
14. C.U. Mordi, M.A. Eleruja, B.A. Taleatu, G.O. Egharevba, A.V. Adedeji, O.O. Akinwunmi, B. Olofinjana, C. Jeynes and E.O.B. Ajayi, *J. Mater. Sci. Technol.*, **25**, 85 (2009).
15. M.Y. Masoomi and A. Morsali, *Coord. Chem. Rev.*, **256**, 2921 (2012); <https://doi.org/10.1016/j.ccr.2012.05.032>
16. L. Zhuo, J. Ge, L. Cao and B. Tang, *Cryst. Growth Des.*, **9**, 1 (2009); <https://doi.org/10.1021/cg070482r>
17. S.J. Bora and B.K. Das, *J. Solid State Chem.*, **192**, 93 (2012); <https://doi.org/10.1016/j.jssc.2012.03.009>
18. R.A. Bepari, Ph.D. Thesis, Gauhati University, Guwahati, India (2014).
19. B.K. Das and J.H. Clark, *Chem. Commun.*, 605 (2000); <https://doi.org/10.1039/b000535p>
20. L.L. Chng, N. Erathodiyil and J.Y. Ying, *Acc. Chem. Res.*, **46**, 1825 (2013); <https://doi.org/10.1021/ar300197s>
21. T. Moritz, J. Reiss, K. Diesner, D. Su and A. Chemseddine, *J. Phys. Chem. B*, **101**, 8052 (1997); <https://doi.org/10.1021/jp970513i>
22. G. Deacon, *Coord. Chem. Rev.*, **33**, 227 (1980); [https://doi.org/10.1016/S0010-8545\(00\)80455-5](https://doi.org/10.1016/S0010-8545(00)80455-5)